Modelling the effect of mechanical remediation on dose rates above radiocesium contaminated land

Alex Malins[1*], Hiroshi Kurikami[1,2], Akihiro Kitamura[1,2], Masahiko Machida[1]

[1]Japan Atomic Energy Agency, Center for Computational Science and e-Systems, 178-4-4 Wakashiba, Kashiwa, Chiba 277-0871, Japan

[2]Japan Atomic Energy Agency, Fukushima Environmental Safety Center, 10-2 Fukasaku, Miharu-machi, Tamura-gun, Fukushima 963-7700, Japan

[*]**Corresponding author**

Dr. Alex Malins

Japan Atomic Energy Agency,

Center for Computational Science and e-Systems,

178-4-4 Wakashiba, Kashiwa, Chiba 277-0871,

Japan

Phone: 0081-7014089980

E. Mail: malins.alex@jaea.go.jp

Abstract

Mechanical strategies for remediating radiocesium contaminated soils, e.g. at farms, schoolyards, gardens or parks, lower air dose rates in one of two characteristic ways. The first is to physically remove radiocesium from the environment, for example by stripping topsoil and sending it for disposal. The second is to redistribute the radiocesium deeper within the ground, e.g. by mixing the topsoil or switching the positions of different soil layers, in order that soil attenuates radiocesium gamma rays before they reach the surface. The amount that air dose rates reduce because of remediation can be calculated using radiation transport methods. This chapter summarizes modelling results for the effect of topsoil removal (with and without recovering with a clean soil layer), topsoil mixing, and soil layer interchange on dose rates. Using measurements of the depth profile of ^{134}Cs and ^{137}Cs activity in soil at unremediated sites across North East Japan, the potential effectiveness of remediation work was estimated considering remediation to different soil depths and at different time lags after the accident. The results show that remediation performance would have been essentially constant irrespective of the time at which it was undertaken in the initial five year period following the fallout.

Keywords: Radiocesium; ^{134}Cs; ^{137}Cs; Mechanical; Remediation; Decontamination; Soil; Topsoil stripping; Soil mixing; Soil layer interchange; Modelling

Contents

1. Introduction

In the aftermath of the March 2011 accident at the Fukushima Daiichi Nuclear Power Plant (FDNPP) the Japanese Government legislated for the remediation of contaminated land across North East Japan (Government of Japan 2011). Remediation efforts were organized separately for the Special Decontamination Area (SDA) surrounding the FDNPP site (the evacuation zone), and the Intensive Contamination Survey Areas (ICSAs) further afield in Iwate, Miyagi, Fukushima, Tochigi, Ibaraki, Gunma, Saitama and Chiba Prefectures. Remediation of the SDA was managed directly by the Government under the auspices of the Ministry of the Environment (MoE), while remediation of the ICSAs was devolved to local municipalities, backed by Government funding and MoE technical assistance (Ministry of the Environment 2013).

Starting in 2011 Japan Atomic Energy Agency (JAEA) conducted research into remediation options for radiocesium contaminated land in the *Decontamination Pilot Project*. Approaches were tested applicable for different land types (forests, farmland, residential areas, public infrastructure etc.) and contamination levels, and generating different wastes as a byproduct. Systematic results on clean-up effectiveness, costs and byproduct volumes from different approaches were summarized in an English language report (JAEA 2015b).

By March 2017 an estimated $24 billion (USD) has been spent remediating the SDA and ICSAs (Ministry of the Environment 2017). One of the most expensive aspects of the program has been the management and storage of large volumes of contaminated topsoil stripped from farmland, residential gardens, public parks, schoolyards etc. (Yasutaka et al. 2013; Yasutaka and Naito 2016). For example the stripping of topsoil down to 5 cm from 85 km^2 of farmland in the SDA alone would have generated over 4,000,000 m^3 of waste, which is a significant proportion of the estimated total of 16,000,000 m^3 of waste generated across Japan by August 2017 (Ministry of the Environment 2017).

The debate on the costs and benefits of the remediation program in Japan should consider not only the averted radiation dose (Miyazaki and Hayano 2017), but also social and economic factors pertinent for the recovery of the contaminated areas (Oughton 2013). It is clearly beneficial however for remediation to maximize contaminant removal (or the reduction in the air dose rate), while minimizing *over-remediation*. This is where soil is stripped or mixed to a depth beyond which there is any further contaminant removal and/or reduction in the air dose rate.

This chapter outlines some previous modelling for the change in air dose rates that occur upon four different mechanical remediation strategies for radiocesium contaminated land (Malins et al. 2016a,b). A new analysis on the effectiveness of remediation is presented eliminating previous modelling assumptions about the depth distribution of radiocesium within soil. The new analysis directly employs measured depth distributions of radiocesium in soil in North East Japan to model remediation performance. The results determine whether remediation performance is affected by the downward migration of radiocesium in soil over the initial five year period following the FDNPP accident.

2. Depth distributions of ^{134}Cs and ^{137}Cs in unremediated soils across North East Japan

One of the pertinent factors that must be considered when designing a remediation program for a site contaminated with radiocesium is the depth distribution of the contamination within the soil prior to remediation. Since December 2011 the Japanese Ministry of Education, Culture, Sports, Science and Technology (MEXT) and the Nuclear Regulation Authority (NRA) have funded the sampling of ^{134}Cs and ^{137}Cs activity depth distributions at unremediated sites within 80 km of FDNPP (Matsuda et al. 2015). At each site a scraper plate apparatus was used to remove soil layers from the surface downwards. The ^{134}Cs and ^{137}Cs activity concentrations in the soil layers (Bq kg^{-1} wet weight) were then measured using High Purity Germanium (HPGe) gamma spectroscopy. The results from eight sampling campaigns running until September 2015 were analyzed in this paper (Table 1). Raw data from the campaigns are published online at JAEA's Database for Radioactive Substance Monitoring Data (JAEA 2015a).

The evolution of the ^{137}Cs depth distribution at a typical site is shown in fig. 1. For the first two sampling campaigns the depth distribution shows a characteristic exponential shape (ICRU 1994). By the third campaign a peak in the ^{137}Cs activity concentration is apparent below the ground surface. The distribution continues to show a peak below the surface through to the eighth sampling campaign.

The trend of the results is for the radiocesium inventory to migrate slowly downwards in the ground over time. Fig. 2(a) shows the mean mass depth of the ^{137}Cs inventory within the ground for both the example site in fig. 1 and for all sites taken collectively. The air dose rate, specifically the ambient dose equivalent rate $\dot{H}^*(10)$ (μSv h^{-1}), at 1 m above the ground tends to decrease over time [fig. 2(b)]. This is predominantly because of radioactive decay and downward migration of the inventory within the soil increasing

the self-shielding of the radiocesium gamma rays (Mikami et al. 2015; Malins et al. 2016b). The two characteristic types of depth distribution seen in the sampling campaigns have been fitted with exponential and hyperbolic secant functions (Matsuda et al. 2015; Malins et al. 2016b):

$$A(\zeta) = A_0 \exp(-\zeta/\beta), \quad (1)$$

$$A(\zeta) = A_0 \cosh(\zeta_0/\beta) \operatorname{sech}(-(\zeta-\zeta_0)/\beta). \quad (2)$$

Here $A(\zeta)$ is the ^{137}Cs activity concentration (Bq kg^{-1}), as a function of the soil mass depth ζ (g/cm^2), A_0 is the activity concentration (Bq kg^{-1}) at the surface, and β and ζ_0 (g/cm^2) are fitting parameters characterizing the penetration of the ^{137}Cs inventory into the ground. In particular ζ_0 is the mass depth of the peak in the activity distribution within the hyperbolic secant model. Note that in Eqs. (1) and (2) mass depths (i.e. the mass of soil between the surface and a given depth below the surface, per unit area) are used instead of physical depths as mass depth is more closely correlated with the amount of shielding provided by soil than physical depth (ICRU, 1994). Fitting the measured depth distributions with these two empirical functions enabled the characterization of the rate of downward migration of the inventories within soil (Matsuda et al. 2015), and a systematic analysis of the effectiveness of different remediation strategies for reducing air dose rates (Malins et al. 2016a).

3. Mechanical remediation strategies

In the main four methods have been employed for the remediation of farms, schoolyards, gardens, parks etc. in North East Japan after the FDNPP accident (Yasutaka et al. 2013; JAEA 2015b; Ministry of the Environment 2015, 2017). The first two methods are variations on topsoil removal [(Fig. 3(a)]. Here the topsoil is stripped down to a set depth and this waste topsoil is sent for disposal. Variations of topsoil stripping include recovering the stripped ground with a clean layer of topsoil brought in from elsewhere (denoted strategy A1), or leaving the stripped ground in a bare state (A2).

Topsoil stripping is effective at lowering dose rates as it segregates the radiocesium contamination from the environment. Another option is to redistribute the contamination deeper within the ground such that the radiocesium gamma rays are attenuated by soil before they reach the surface. The soil layer interchange method is an example of the latter option [A3, Fig. 3(b)]. Soil layer interchange involves first digging out a layer of topsoil and placing this to one side. Then a layer of subsoil is excavated from the pit that has been created. The pit is then refilled first with the soil that was initially topsoil, and finally to the surface with the soil that was initially subsoil.

The fourth mechanical remediation method is topsoil mixing [A4, Fig. 3(c)]. In this method the topsoil is mixed down to a set depth using a rotovator or a plow pulled by a tractor. A notable disadvantage of soil layer interchange and topsoil mixing methods (A3 and A4) over topsoil stripping (A1 and A2) is that the radiocesium still remains within the environment after remediation, albeit at a greater soil mass depth below the surface. This may potentially affect the viability of agricultural products produced on farmland remediated by methods A3 or A4.

Yasutaka et al. (2013) estimated the total cost of remediating the agricultural land in the SDA by topsoil stripping (A1 and A2) as between 1022 billion and 2270 billion Japanese yen (~$10 billion to $23 billion USD). This compares with 62 billion yen (~$620 million USD) for the soil layer interchange method (A3), and 7 billion yen (~$70 million USD) for the soil mixing method (A4). Topsoil stripping is thus one to two orders of magnitude more expensive than the soil layer interchange and topsoil mixing remediation strategies.

4. Remediation effect on air dose rates (modelling of empirical activity depth distributions)

Malins et al. (2016a) performed a systematic analysis of the change that occurs in the 1 m ambient dose equivalent rate [$\dot{H}^*(10)$] upon remediation by each of the four mechanical strategies (A1 to A4) using the results of Monte Carlo radiation transport calculations. Simplified land geometry was modelled consisting of an infinite slab of soil and air (Malins et al. 2016b). The ^{134}Cs and ^{137}Cs activity concentration over the land surface was assumed to be uniform in the initial state prior to remediation, i.e. constant Bq/m^2. The initial radiocesium depth distribution was modelled as either an exponential [Eq. (1)] or the hyperbolic secant [Eq. (2)] distribution. This method of calculating $\dot{H}^*(10)$ using an approximated environmental geometry and radiocesium distribution was shown to give reasonably accurate results when its predictions were compared against actual measurements of $\dot{H}^*(10)$ at unremediated sites within 80 km of FDNPP (Malins et al. 2016b).

Dose rates after remediation were calculated by altering the radiocesium depth distribution within a square area of land that was modelled as having been remediated by one strategy (A1, A2, A3 or A4). Taking the topsoil mixing method as an example, the radiocesium distribution in the mixed topsoil layer was modelled as a homogeneous distribution throughout the layer (i.e. perfect mixing of the soil). Results from this strategy for modelling remediation were consistent with measured reductions in air dose

rates upon remediation of test sites in the Decontamination Pilot Project (JAEA 2015b; Malins et al. 2016a).

The effect that various parameters have upon the amount that dose rates decrease were examined systematically. Variables considered included the initial distribution of radiocesium into the ground prior to remediation, by varying β and ζ_0 in Eqs. (1) and (2), the area of land that was remediated, and the mass depth to which soil was remediated.

The performance of each remediation strategy was characterized in terms of the ratio of the ^{134}Cs (^{137}Cs) component of $\dot{H}^*(10)$ post-remediation to its initial value:

$$R_{134} = {}^{134}_{r}\dot{H}^*(10)/{}^{134}_{i}\dot{H}^*(10), \quad (3)$$

$$R_{137} = {}^{137}_{r}\dot{H}^*(10)/{}^{137}_{i}\dot{H}^*(10). \quad (4)$$

Here the subscripts *r* and *i* denote the remediated and initial air dose rates, respectively. R_{134} and R_{137} are termed *residual dose rate factors*. As the residual dose rate factors represent the relative change in the radiocesium components of $\dot{H}^*(10)$ rather than $\dot{H}^*(10)$ as a whole, they apply generally rather than being specific to any particular remediation site. Assuming the natural background component of the air dose rate [$^{nat}\dot{H}^*(10)$] at a given site is unchanged by remediation, the air dose rate after remediation is:

$${}_{r}\dot{H}^*(10) = R_{134}\times{}^{134}_{i}\dot{H}^*(10)+R_{137}\times{}^{137}_{i}\dot{H}^*(10)+{}^{nat}\dot{H}^*(10). \quad (5)$$

Fig. 4 shows residual dose rate factors for remediation of soil by methods A1 to A4. The initial radiocesium depth distribution was modelled an exponential distribution with β = 2.0 g/cm^2. The residual dose rate factors for ^{134}Cs and ^{137}Cs coincide as the energies of the primary gamma rays emitted by these radioisotopes are comparable.

In general the topsoil stripping methods (A1 and A2, top panels of fig. 4) are more effective for reducing air dose rates than the soil layer interchange (A3, lower left panel of Fig. 4) or topsoil mixing (A4, lower right panel of fig. 4) methods. This is clear when comparing data points between the panels at equal remediation mass depth and remediated land area.

The residual dose rate factors for the topsoil removal methods plateau out for remediation mass depths greater than ~10 g/cm^2. Essentially all the radiocesium has been removed from remediation zone upon remediation to these mass depths. Further removal of topsoil thus conveys no further reduction in the air dose rate.

The reason that the residual dose rate factors plateau at values above zero is because of radiocesium that remains outside the remediated area of land. Cesium-134 and ^{137}Cs gamma rays have a mean free path in air on the order of 100 m (Malins et al. 2015), and

very large areas need to be remediated to completely eliminate this residual radiocesium component of the dose rate. This effect can be seen by examining the colored lines in fig. 4. Cooler colors indicate increasingly larger areas of land that were modelled as remediated. The remediation performance increases (lower residual dose rate factors) with the size of the remediated area.

Topsoil removal and recovering with a clean soil layer (A1) only outperforms topsoil removal alone (A2) within a narrow range of remediation mass depths (between 0 and 10 g/cm^2). In this range recovering with a clean soil layer leads to slightly lower residual dose rate factors than without replacing the stripped soil. This is because of shielding provided by the covering layer of clean soil. However the effect is small, and moreover there is no radiological benefit of recovering with a clean soil layer for larger remediation mass depths, as the amount of radiocesium remaining inside the remediated zone is negligible.

The soil layer interchange method (A3) is more effective than topsoil mixing (A4) given equal remediation parameters. This is because, given equal remediation mass depths, soil layer interchange redistributes the radiocesium more deeply within the ground than topsoil mixing, resulting in a larger shielding effect by the soil.

The curves of the residual dose rate factors for methods A3 and A4 decrease more slowly with increasing remediation mass depth than for the topsoil removal methods. As a consequence larger remediation mass depths are necessary with soil layer interchange and topsoil mixing to achieve the same residual dose rate factor given by topsoil stripping. Taking the top red curve in Fig. 4 as an example (12.5 m by 12.5 m remediation area), topsoil stripping to 10 g/cm^2 (A1 or A2) results in a residual dose rate factor of 0.4 (i.e. 60% reduction in the radiocesium component of [$\dot{H}$*(10)]. The remediation mass depth required to give a corresponding result with soil layer interchange is on the order of 80 g/cm^2, and even larger for topsoil mixing.

Malins et al. (2016a) presented further results on residual dose rate factors. When the initial depth distribution was modelled as an exponential function, residual dose rate factors were calculated for relaxation mass depths of β = 1.0 and 5.0 g/cm^2, in addition to β = 2.0 g/cm^2 (fig. 4). When modelling the initial depth distribution with the hyperbolic secant function, both β and ζ_0 were varied between 1.0 and 5.0 g/cm^2.

The effect of migration of the radiocesium inventory downwards in soil over time on the performance of remediation was investigated by considering different possible rates of evolution of the radiocesium depth distribution. Downward migration of radiocesium

was modelled by increasing the relaxation mass depth (β) of the exponential distribution in Eq. (1). Relaxation mass depths applicable at different lags post fallout were drawn from values published in ICRU (1994), based on a global literature search, and by reverse modelling of the dose rate attenuation factors derived by Likhtarev et al. (2002) for sites in Ukraine affected by Chernobyl accident fallout.

Fig. 5 shows the results of this analysis, considering up to 20 years migration of radiocesium within soil following its deposition. The results are sensitive to the model chosen for the evolution of the radiocesium depth profile over time, i.e. the speed at which downward migration occurs. With the faster scenarios for the downward migration (ICRU 53 fast and medium models in fig. 5), the performance of remediation decreases the later it is undertaken after the initial contamination event. This is indicated by the increase in the ^{137}Cs residual dose rate factors in fig. 5. One option to recover the performance of remediation undertaken at late times after the initial contamination event would be to increase the (mass) depth to which soil is remediated.

5. Remediation modelling using measured activity depth profiles

A limitation of the results described in the previous section is the assumption that the initial depth distribution of the radiocesium takes a perfectly exponential or hyperbolic secant form. In reality radiocesium depth distributions always differ from these empirical models. This limitation may be significant as long tails have been observed in depth distributions of radiocesium fallout worldwide (Antonopoulos-Domis et al. 1995; Matsuda et al. 2015; Takahashi et al. 2015). The long tails are not well characterized by a single exponential function (Kurikami et al. 2017).

A study was therefore undertaken of the effectiveness of remediation without resorting to an empirical assumption about the nature of the radiocesium depth distribution prior to remediation. Data on depth distributions at the unremediated sites within 80 km of FDNPP (Table 1) were used to model the initial radiocesium depth distribution prior to remediation. In particular the thickness, mass, and ^{134}Cs and ^{137}Cs activity concentration of each soil layer was used to define a step-wise activity distribution. Remediation was then modelled within a 37.5 m by 37.5 m area of land using methods A1 to A4.

Topsoil stripping (A1 and A2) was modelled down to physical depths of 3, 5 and 7 cm below the surface. The corresponding remediation depths for soil layer interchange and topsoil mixing were 10, 20 and 30 cm. The post-remediation distributions for the radiocesium inventory, and other applicable modelling factors, were defined in an identical manner to Malins et al. (2016a).

The results are presented in Fig. 6, with individual panels showing data for methods A1 to A4. Remediation performance was assessed in terms of the ratio of total radiocesium component (^{134}Cs and ^{137}Cs) of $\dot{H}^*(10)$ post-remediation to its initial value prior to remediation. Each data point represents the mean of all residual dose rate factors from one soil sampling campaign. The data are plotted as a function of the number of years elapsed since March 2011.

The overarching result is that the residual dose rate factors show little sensitivity to the time point at which remediation is undertaken in the initial five year period following the fallout. Although the radiocesium inventory did tend to migrate downwards within the soil over this period [fig. 2(a)], the results of fig. 6 indicate that migration is insignificant over the scale of the remediation depths.

The possible exceptions are the results for topsoil removal down to 3 cm (solid lines and circle markers, fig. 6(a) and (b)). Here the residual dose rate factors increase by a small amount with increasing number of years after the fallout. This indicates that a proportion of the radiocesium inventory migrated downwards below 3 cm over the five year period. Remediation by topsoil removal in the latter years of the five year period therefore does not remove the entire radiocesium inventory. The residual dose rate after remediation is thus larger than if remediation had been undertaken at an earlier time.

There is only a small difference in the performance of the two topsoil removal methods when stripping 5 cm or more of topsoil [cf. fig. 6(a) and (b)]. This reinforces the previous conclusion that once the majority of the radiocesium inventory has been removed from the environment, i.e. the inventory of the top few centimeters of topsoil, there are diminishing returns from stripping further topsoil or by recovering with a clean soil layer.

By comparing figs. 5 and 6 it is clear that the trend of the residual dose rate factors for North East Japan for the first five years after the contamination fallout are most consistent with the ICRU 53 slow and Likhtarev et al. models in fig. 5. Therefore, excluding the case of topsoil stripping down to 3 cm alone, there is no indication that increasing the remediation depth over the first five years following the FDNPP accident was necessary to maintain remediation performance.

The performance of remediation undertaken five or more years after the FDNPP accident will depend on the development of the radiocesium depth profile within the soil. It is known that cesium binds strongly to clay minerals in soil (Okumura et al. 2013; Mukai et al. 2014; Fuller et al. 2015). This suggests that future changes to the

radiocesium depth distribution will depend on natural biological and physical mixing of the soil, rather than physiochemical migration of the radiocesium ions (Kurikami et al. 2017). Past experience of Chernobyl fallout in Eastern Europe (IAEA 2006), and Mayak contamination of the Techa River, South Ural Mountains, Russia (Akleyev and Kisselyov 2002) has shown radiocesium tends to remain in the upper 20 cm of soil, even 35 years after the initial contamination event. This suggests mechanical soil remediation will remain a viable strategy for lowering air dose rates in as yet unremediated areas in North East Japan over the coming years.

6. Conclusions

Mechanical remediation of radiocesium contaminated soil was one of the most expensive aspects of the remediation program undertaken in Japan after the FDNPP accident in 2011. This chapter summarized modelling work for the relationship between different mechanical remediation strategies for radiocesium contaminated soil and reductions in air dose rates. By using a modelling approach it was possible to quickly and cheaply quantify the effect of various factors on the performance of the remediation work, including the amount of soil that is remediation (both in terms of land area and soil depth) and the initial depth distribution of radiocesium in soil.

Topsoil removal, with or without recovering with a clean soil layer, tends to be more effective at lowering air dose rates than either soil layer interchange or soil mixing. This is because radiocesium is removed and separated from the environment with the former strategies. In order to attain the levels of dose rate reduction achieved by stripping circa 10 g/cm^2 of topsoil, it is necessary to remediate down to much larger soil mass depths with either the soil layer interchange or topsoil mixing methods.

Radiocesium activity depth distributions from North East Japan were modelled to determine the effect of downward migration of radiocesium in soil on remediation performance. The results suggest remediation performance is independent of the time at which it is undertaken within five years from March 2011. The exception to this conclusion was topsoil stripping (A1 or A2) to 3 cm. Migration of radiocesium below 3 cm depth in the initial five year period means topsoil stripping to 3 cm becomes less effective the later it is undertaken.

Acknowledgements

We thank S. Nakama, K. Saito and K. Miyahara for their advice and assistance to this work.

References

Akleyev AV, Kisselyov MF (2002) Medical-biological and ecological impacts of radioactive contamination of the Techa River. Fregat, Chelyabinsk.

Antonopoulos-Domis M, Clouvas A, Hiladakis A, Kadi S (1995) Radiocesium distribution in undisturbed soil: measurements and diffusion-advection model. Health Phys 69:949–953.

Fuller AJ, Shaw S, Ward MB, Haigh SJ, Mosselmans JFW, Peacock CL, Stackhouse S, Dent AJ, Trivedi D, Burke IT (2015) Caesium incorporation and retention in illite interlayers. Appl Clay Sci 108:128–134.

Government of Japan (2011) Act on Special Measures concerning the Handling of Environment Pollution by Radioactive Materials Discharged by the NPS Accident Associated with the Tohoku District-Off the Pacific Ocean Earthquake That Occurred on March 11, 2011

IAEA (2006) STI/PUB/1239: Environmental consequences of the Chernobyl accident and their remediation: 20 years of experience. Report of the Chernobyl Forum Expert Group 'Environment'. URL http://www-pub.iaea.org/MTCD/publications/PDF/Pub1239_web.pdf

ICRU (1994) ICRU 53: Gamma-Ray Spectrometry in the Environment.

JAEA (2015a) Database for Radioactive Substance Monitoring Data-Depth Distribution in Soil. URL http://emdb.jaea.go.jp/emdb/en/

JAEA (2015b) JAEA-Review 2014-051: Remediation of Contaminated Areas in the Aftermath of the Accident at the Fukushima Daiichi Nuclear Power Station: Overview, Analysis and Lessons Learned Part 1: A Report on the 'Decontamination Pilot Project'. Tech. Rep. March, Japan Atomic Energy Agency, DOI 10.11484/jaea-review-2014-051.

Kurikami H, Malins A, Takeishi M, Saito K, Iijima K (2017) Coupling the advection-dispersion equation with fully kinetic reversible/irreversible sorption terms to model radiocesium soil profiles in Fukushima Prefecture. J Environ Radioact 171:99–109.

Likhtarev IA, Kovgan LN, Jacob P, Anspaugh LR (2002) Chernobyl accident: retrospective and prospective estimates of external dose of the population of Ukraine. Health Phys 82:290–303.

Malins A, Okumura M, Machida M, Takemiya H, Saito K (2015) Fields of View for Environmental Radioactivity. In: Proceedings of the International Symposium on Radiological Issues for Fukushima's Revitalized Future, pp 28–34.

Malins A, Kurikami H, Kitamura A, Machida M (2016a) Effect of remediation parameters on in-air ambient dose equivalent rates when remediating open sites with radiocesium-contaminated soil. Health Phys 111:357–366.

Malins A, Kurikami H, Nakama S, Saito T, Okumura M, Machida M, Kitamura A (2016b) Evaluation of ambient dose equivalent rates influenced by vertical and horizontal distribution of radioactive cesium in soil in Fukushima Prefecture. J Environ Radioact 151:38–49.

Matsuda N, Mikami S, Shimoura S, Takahashi J, Nakano M, Shimada K, Uno K, Hagiwara S, Saito K (2015) Depth profiles of radioactive cesium in soil using a scraper plate over a wide area surrounding the Fukushima Dai-ichi Nuclear Power Plant, Japan. J Environ Radioact 139:427–434.

Mikami S, Maeyama T, Hoshide Y, Sakamoto R, Sato S, Okuda N, Sato T, Takemiya H, Saito K (2015) The air dose rate around the Fukushima Daiichi Nuclear Power Plant: its spatial characteristics and temporal changes until December 2012. J Environ Radioact 139:250–259.

Ministry of the Environment (2013) Decontamination Guidelines. Tech. rep., URL http://josen.env.go.jp/en/framework/pdf/decontamination guidelines 2nd.pdf.

Ministry of the Environment (2015) FY2014 Decontamination Report. Tech. rep., URL http://josen.env.go.jp/en/cooperation/pdf/decontamination report1503 01.pdf.

Ministry of the Environment (2017) Progress on Off-site Cleanup and Interim Storage in Japan (August 2017). Tech. Rep.

Miyazaki M, Hayano R (2017) Individual external dose monitoring of all citizens of Date City by passive dosimeter 5 to 51 months after the Fukushima NPP accident (series): II. Prediction of lifetime additional effective dose and evaluating the effect of decontamination on individual. J Radiol Prot 37:623–634.

Mukai, H, Hatta, T, Kitazawa, H, Yamada, H, Yaita, T, Kogure, T, 2014. Speciation of radioactive soil particles in the Fukushima contaminated area by IP autoradiography and microanalyses. Environ Sci Technol 48:13053–13059.

Okumura M, Nakamura H, Machida M (2013) Mechanism of strong affinity of clay minerals to radioactive cesium: First-principles calculation study for adsorption of cesium at frayed edge sites in muscovite. J Phys Soc Jpn 82:033802.

Oughton DH (2013) Social and ethical issues in environmental remediation projects. J Environ Radioact 119:21–5.

Takahashi J, Tamura K, Suda T, Matsumura R, Onda Y (2015) Vertical distribution and temporal changes of (137)Cs in soil profiles under various land uses after the Fukushima Dai-ichi Nuclear Power Plant accident. J Environ Radioact 139:351–361.

Yasutaka T, Naito W (2016) Assessing cost and effectiveness of radiation decontamination in Fukushima Prefecture, Japan. J Environ Radioact 151:512–520.

Yasutaka T, Naito W, Nakanishi J (2013) Cost and effectiveness of decontamination strategies in radiation contaminated areas in Fukushima in regard to external radiation dose. PLoS ONE 8(9):e75308.

Figure Captions

Figure 1: Evolution of the ^{137}Cs depth distribution in the grounds of a religious assembly hall, 5 km south of Koriyama City, Fukushima Prefecture.

Figure 2: (a) Mean mass depth of the ^{137}Cs inventory across all unremediated sites and at the assembly hall 5 km south of Koriyama City. (b) Change in the air dose rate [$\dot{H}$*(10)] measured at 1 m.

Figure 3: Mechanical remediation strategies for radiocesium contaminated soil. Photos reproduced from JAEA (2015b).

Figure 4: Residual dose rate factors as a function of remediation mass depth and the size of the remediated area, given an initially exponential radiocesium depth distribution (β = 2:0 g/cm^2). Solid lines indicate results for ^{137}Cs, while dashed lines are those for ^{134}Cs. The legend in the upper right panel lists the various sizes of the remediated area. Figure adapted from Malins et al (2016a).

Figure 5: The change in ^{137}Cs residual dose rate factors under four different models for the migration of radiocesium downwards in soil over time. In all cases the modelled area of remediated land was 37.5 m by 37.5 m. The remediation mass depths were fixed at 6.7 g/cm^2 for strategies A1 and A2, 40.3 g/cm^2 for strategy A3, and 33.8 g/cm^2 for A4. Figure adapted from Malins et al (2016a).

Figure 6: Mean residual dose rate factors for the radiocesium component of $\dot{H}$*(10) upon modelled remediation of with 80 km of FDNPP. Different panels show results for A1 to A4 methods of remediation. Lines and markers represent different physical depths to which the soil was remediated (see legends). Error bars show plus/minus one standard deviation from the mean. In all cases the size of remediated area was 37.5 m by 37.5 m.

Table 1: Details of the eight soil sampling campaigns for the depth distribution of ^{134}Cs and ^{137}Cs at unremediated sites within 80 km of FDNPP.

Campaign	**Period**	**No. sites analyzed**	**Mean ^{137}Cs mass depth (g/cm^2)**	**Mean $\dot{H}^*(10)$ at 1 m ($\mu Sv\ h^{-1}$)**
1	Dec 12-22, 2011 and Apr 17-19, 2012	83	0.99	0.60a
2	Aug 21 to Sep 26, 2012	81	1.09	0.51
3	Nov 26 to Dec 21, 2012	82	1.25	0.47
4	Jun 4-27, 2013	82	1.35	0.49
5	Oct 28 to Nov 29, 2013	80	1.58	0.40
6	Jul 14-24, 2014	76	1.81	0.36
7	Nov 4-13, 2014	76	1.70	0.35
8	Aug 24 to Sep 25, 2015	72	1.96	0.22

[a]Mean of measurements from 41 sites only [$\dot{H}^*(10)$ was not measured at all sites in campaign 1].

Figure 1:

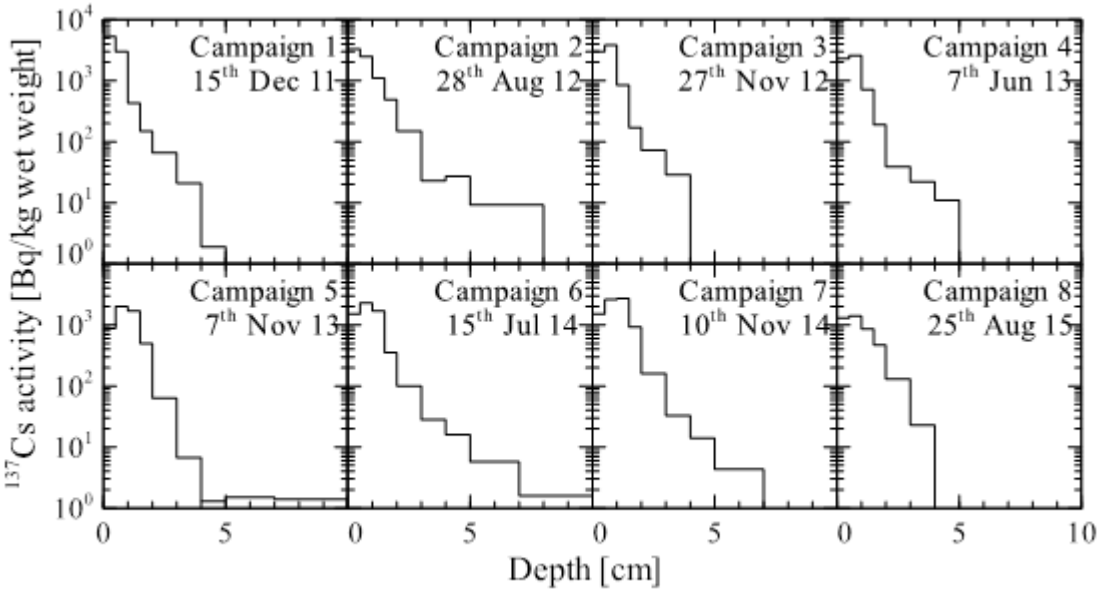
Campaign 1
15th Dec 11
Campaign 2
28th Aug 12
Campaign 3
27th Nov 12
Campaign 4
7th Jun 13
Campaign 5
7th Nov 13
Campaign 6
15th Jul 14
Campaign 7
10th Nov 14
Campaign 8
25th Aug 15
137Cs activity [Bq/kg wet weight]
Depth [cm]

Figure 2:

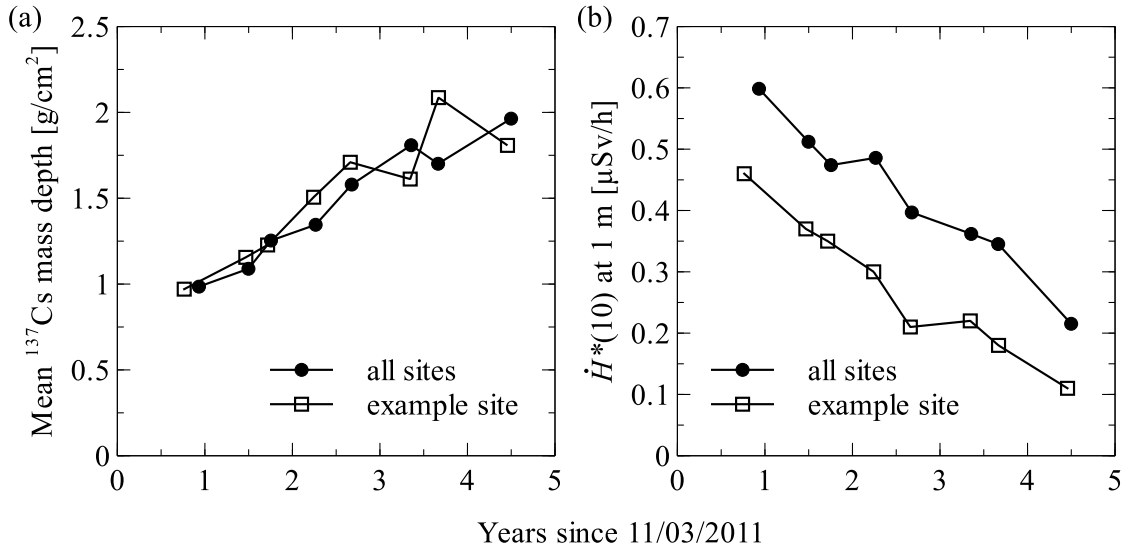
(a)
Mean ^{137}Cs mass depth [g/cm^2]
2.5
2
1.5
1
0.5
0
all sites
example site
(b)
$\dot{H}$*(10) at 1 m [µSv/h]
0.7
0.6
0.5
0.4
0.3
0.2
0.1
0
all sites
example site
0
1
2
3
4
5
Years since 11/03/2011

Figure 3:

(a) Topsoil stripping
(A1 recovered & A2 bare)

(b) Soil layer interchange
(A3)

(c) Topsoil mixing
(A4)

Figure 4:

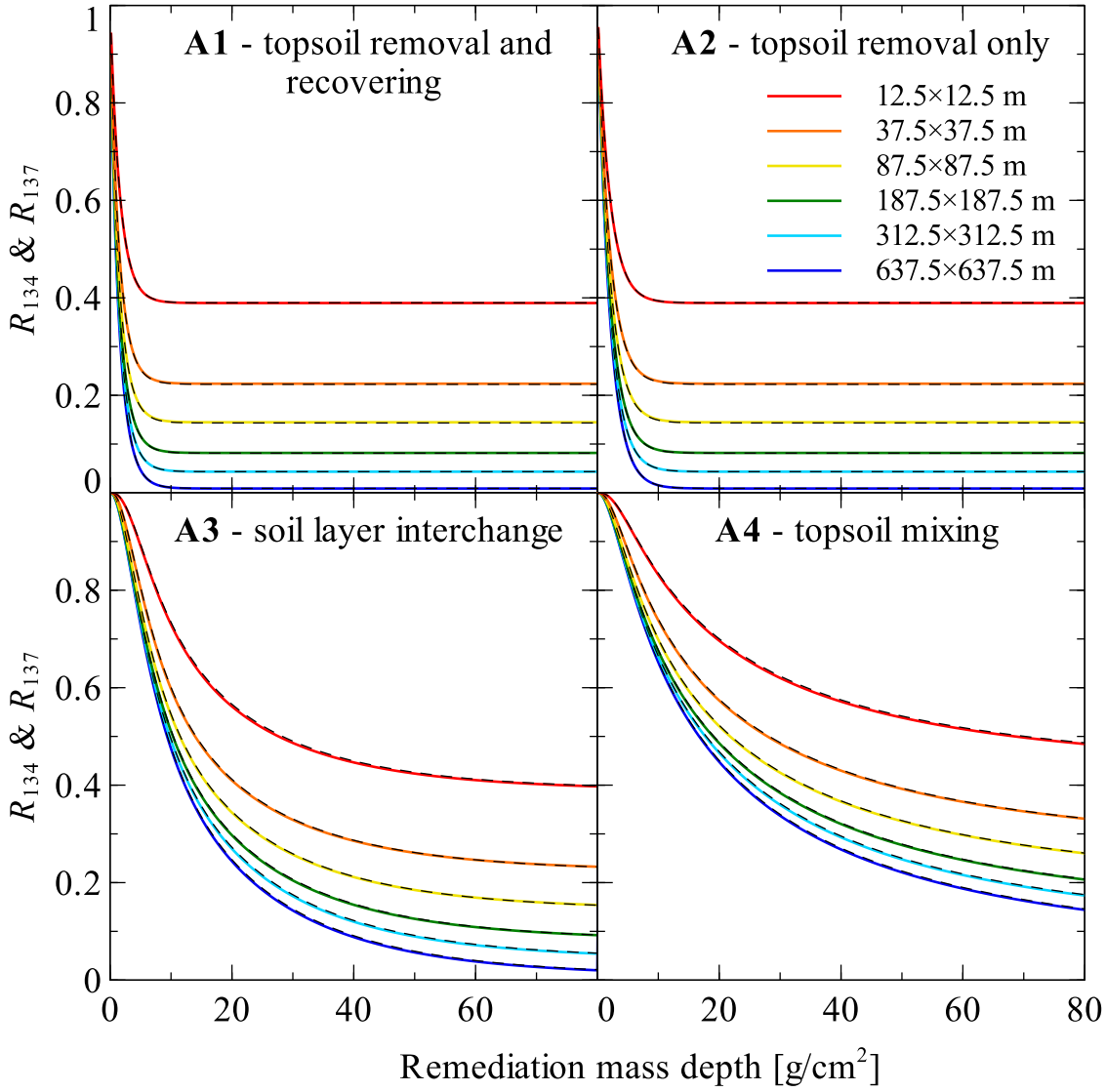
A1 - topsoil removal and recovering
A2 - topsoil removal only
A3 - soil layer interchange
A4 - topsoil mixing
12.5×12.5 m
37.5×37.5 m
87.5×87.5 m
187.5×187.5 m
312.5×312.5 m
637.5×637.5 m
R134 & R137
Remediation mass depth [g/cm2]
0
0.2
0.4
0.6
0.8
1
0
20
40
60
80

Figure 5:

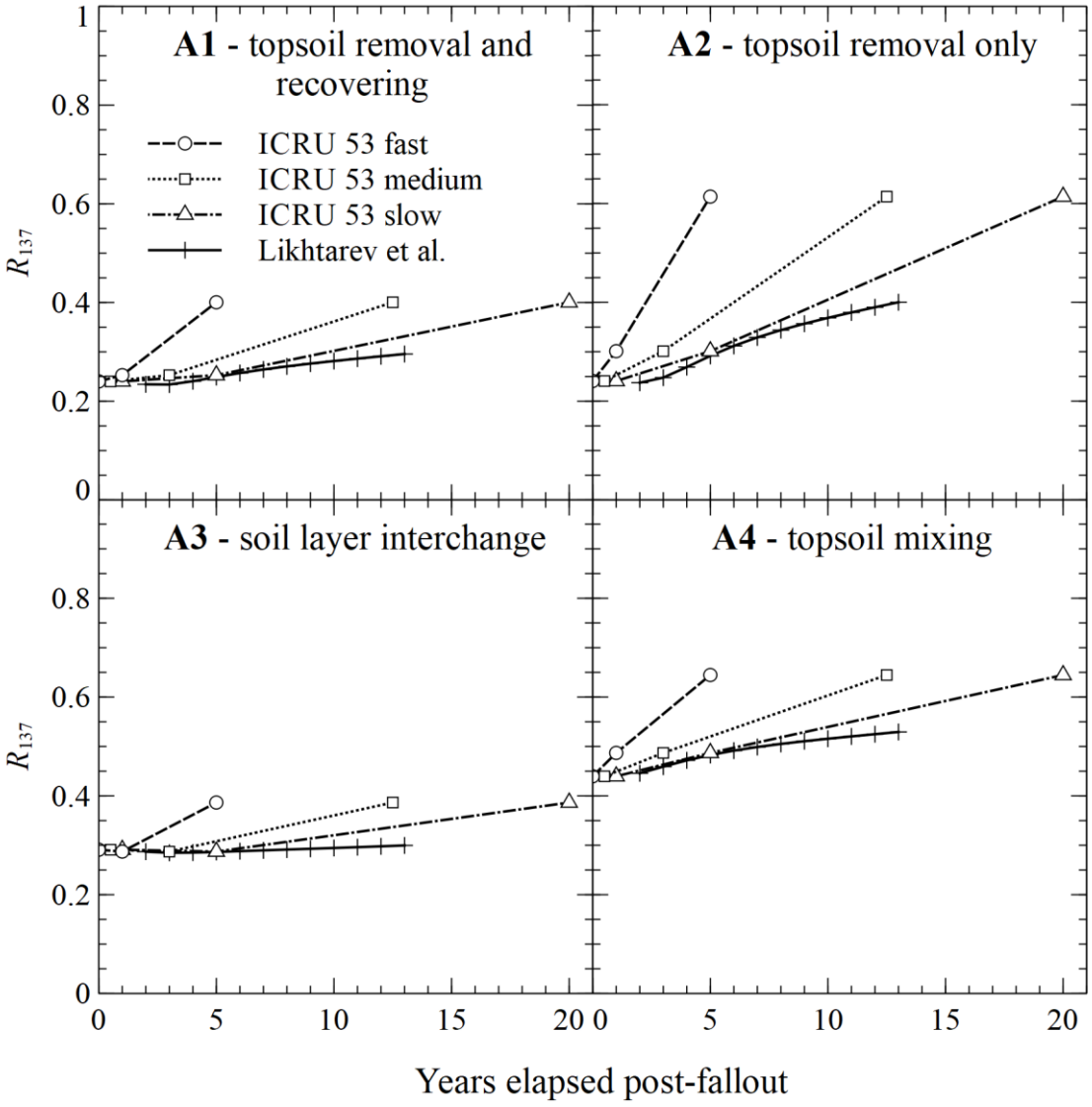
A1 - topsoil removal and recovering
ICRU 53 fast
ICRU 53 medium
ICRU 53 slow
Likhtarev et al.
A2 - topsoil removal only
A3 - soil layer interchange
A4 - topsoil mixing
R_{137}
Years elapsed post-fallout
0
0.2
0.4
0.6
0.8
1
0
5
10
15
20

Figure 6:

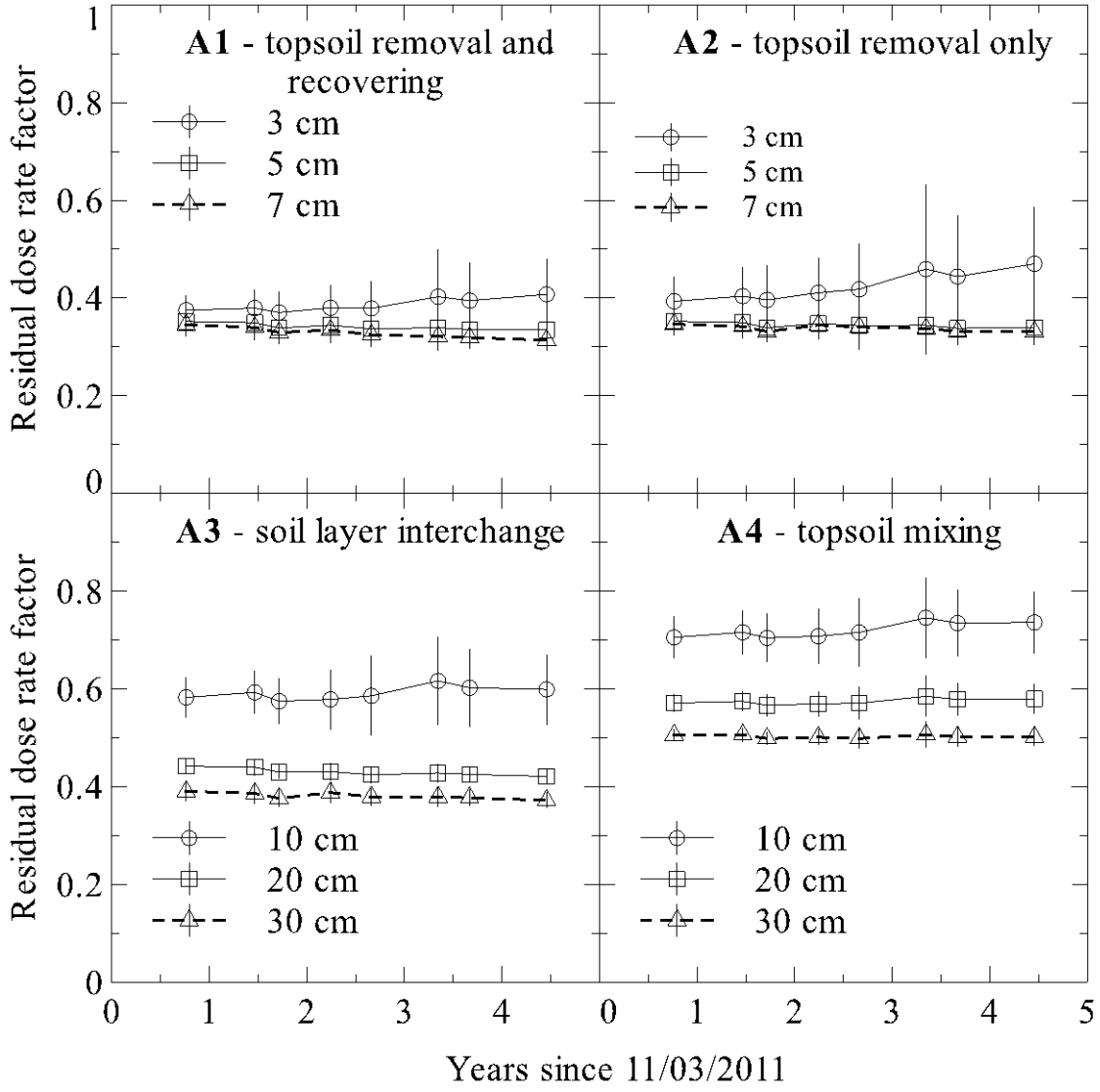
A1 - topsoil removal and recovering
3 cm
5 cm
7 cm
A2 - topsoil removal only
3 cm
5 cm
7 cm
A3 - soil layer interchange
10 cm
20 cm
30 cm
A4 - topsoil mixing
10 cm
20 cm
30 cm
Residual dose rate factor
Residual dose rate factor
Years since 11/03/2011